PHYSICAL REVIEW D **91,** 033007 (2015)

Lepton flavor violation in the supersymmetric seesaw model after the LHC 8 TeV run

Toru Goto[*] and Yasuhiro Okada[†]

Theory Center, IPNS, KEK, 1-1 Oho, Tsukuba, Ibaraki 305-0801, Japan and Department of Particle and Nuclear Physics, Graduate University for Advanced Studies (Sokendai), 1-1 Oho, Tsukuba, Ibaraki 305-0801, Japan

Tetsuo Shindou[‡]

Division of Liberal Arts, Kogakuin University, 1-24-2 Shinjuku, Tokyo 163-8677, Japan

Minoru Tanaka[§]

Department of Physics, Graduate School of Science, Osaka University, Toyonaka, Osaka 560-0043, Japan

Ryoutaro Watanabe[‖]

Center for Theoretical Physics of the Universe, Institute for Basic Science (IBS), Daejeon 305-811, Republic of Korea

(Received 11 December 2014; published 26 February 2015)

We study the lepton flavor violation in the supersymmetric seesaw model, taking into account recent experimental improvements, especially for the Higgs boson mass measurement, direct searches of superpartners, and the rare decay of $B_s \to \mu^+\mu^-$ at the LHC; the neutrino mixing angle of θ_{13} in the neutrino experiments; and the search of $\mu \to e\gamma$ in the MEG experiment. We obtain the latest constraints on the parameters in the supersymmetry-breaking terms and study the effect on the lepton-flavor-violating decays of $\tau \to \mu\gamma$ and $\mu \to e\gamma$. In particular, we consider two kinds of assumption on the structures in the Majorana mass matrix and the neutrino Yukawa matrix. In the case of the Majorana mass matrix proportional to the unit matrix, allowing nonvanishing CP-violating parameters in the neutrino Yukawa matrix, we find that the branching ratio of $\tau \to \mu\gamma$ can be larger than 10^{-9} within the improved experimental limit of $\mu \to e\gamma$. We also consider the neutrino Yukawa matrix that includes the mixing only in the second and third generations, and we find that a larger branching ratio of $\tau \to \mu\gamma$ than 10^{-9} is possible while satisfying the recent constraints.

DOI: 10.1103/PhysRevD.91.033007 PACS numbers: 14.60.Pq, 12.60.Jv, 13.35.-r

I. INTRODUCTION

The discovery of neutrino oscillations [1] means that lepton flavors are not conserved and that the minimal standard model (SM) with massless neutrinos must be extended. The seesaw mechanism is a simple and attractive extension to introduce the neutrino masses [2]. Similarly to the quark sector in the SM, a new additional Yukawa matrix for right-handed neutrinos induces lepton flavor violations (LFVs) in the charged lepton sector. In this simple extension, however, the LFV processes only occur via loop including a neutrino and are suppressed by small neutrino masses. If this is the case, it is practically impossible to observe the LFV except for the neutrino oscillations.

An interesting extension is to impose supersymmetry (SUSY) on the seesaw mechanism [3]. The LFV processes are induced via loop contributions from charged sleptons and sneutrinos whose masses are expected not to be far away from the electroweak scale. There is a possibility to enhance the LFV processes so that they can be measured in near future experiments.

In recent years, there have been great experimental developments, and the allowed ranges of the model parameters have significantly changed. The most important development is that a Higgs boson was discovered from a diphoton decay [4,5] in July 2012 at the Large Hadron Collider (LHC), whose mass is now found to be about 126 GeV [6,7]. Superpartners of the SM particles have not been discovered yet, and the lower mass bound of colored superpartners is about 1 TeV after the 8 TeV run of the LHC [8,9]. Flavor experiments also give us improved constraints on new physics. For B physics, the recent improvement of $\mathcal{B}(b \to s\gamma)$ and the evidence of $B_s \to \mu^+\mu^-$ have impacts on the model [10–14]. For the lepton sector, the neutrino mixing angles introduced in the Pontecorvo-Maki-Nakagawa-Sakata (PMNS) matrix [15] have been precisely determined by many kinds of neutrino experiments

[*]tgoto@post.kek.jp
[†]yasuhiro.okada@kek.jp
[‡]shindou@cc.kogakuin.ac.jp
[§]tanaka@phys.sci.osaka-u.ac.jp
[‖]wryou1985@ibs.re.kr

summarized in Ref. [16], including the recent improvements [17–21] for $\sin\theta_{13}$. In addition, bounds on the branching ratios of LFV processes for $\mu \to e\gamma$ [22] and $\tau \to (\mu, e)\gamma$ [23,24] have been strengthened.

As a consequence of the Higgs boson discovery and the limit on SUSY particle masses, we expect that the scale of SUSY breaking is very high, or the A-term, a trilinear scalar interaction term in the stop sector, is tuned to reproduce the correct Higgs boson mass. In the supersymmetric seesaw model, LFV processes depend on both the structure of the neutrino sector and SUSY model parameters. In the previous work [25] in 2008, the supersymmetric seesaw model of type I was studied. In general, $\tau \to \mu\gamma$ is severely constrained by the experimental bound on $\mu \to e\gamma$ because their decay branching ratios are related, but it is shown that the ratio $\mathcal{B}(\tau \to \mu\gamma)/\mathcal{B}(\mu \to e\gamma)$ can be enhanced in several cases of the flavor structure of the seesaw sector. For example, a large enhancement of the ratio could occur with the simplest structure, in that the Majorana mass matrix is proportional to the unit matrix and the neutrino Yukawa matrix is real provided that the neutrino mixing angle of θ_{13} is zero and the neutrino masses are inversely hierarchical. In addition, such an enhancement is also found if the neutrino Yukawa matrix is assumed to have a mixing only between the second and third generations for both cases of the normal and inverted hierarchies of the neutrino masses. Another enhancement mechanism is also discussed in Ref. [26] by considering the effect of the CP-violating parameters in the neutrino Yukawa matrix. There are many other studies for the LFV in the SUSY seesaw models [27], taking several constraints of the day into account. However, these studies have to be reexamined due to the above experimental improvements. Recent studies have been done for $\mu \to e\gamma$ in the case of a simple assumption on the neutrino Yukawa matrix and Majorana mass matrix in Refs. [28,29]. The tau and muon LFV decays have recently been studied in the model embedded in an SO(10) grand unified theory (GUT) [30].

In the present work, we investigate both tau and muon LFV decays in the supersymmetric seesaw model of type I. We take the universal soft SUSY breaking and assume several specific structures on the neutrino Yukawa matrix and the Majorana mass matrix. In order to find how much the latest constraints change the previous results in Refs. [25,26], we first determine allowed regions of SUSY parameters. Then, we analyze the LFV decays $\tau \to \mu\gamma$ and $\mu \to e\gamma$. As a result, we see that the enhancement of $\mathcal{B}(\tau \to \mu\gamma)/\mathcal{B}(\mu \to e\gamma)$ is unlikely to occur for the simplest structure with the degenerate Majorana mass matrix and the real neutrino Yukawa matrix because of the sizable value of θ_{13}. On the other hand, in the case of degenerate Majorana mass together with CP-violating parameters in the neutrino Yukawa matrix, we find that an enhancement of $\mathcal{B}(\tau \to \mu\gamma)/\mathcal{B}(\mu \to e\gamma)$ is possible. We also consider the neutrino Yukawa matrix that includes the mixing only in the second and third generations, and find that the branching ratio of $\tau \to \mu\gamma$ can be as large as 10^{-9}. These results imply that there is a good possibility for the tau LFV decay to be measured in the SuperKEKB/Belle II [31] experiment in addition to the muon LFV decay in the upgraded MEG experiment (MEG II) [32].

This article is organized as follows: In Sec. II, we review the supersymmetric seesaw model and summarize parametrizations for the seesaw sector. We describe our analysis method to evaluate flavor signals in Sec. III. We present numerical results in Sec. IV. Summary and conclusion are given in Sec. V.

II. SUPERSYMMETRIC SEESAW MODEL

A. Overview of the model

In this section, we briefly review the supersymmetric seesaw model and summarize its features. As is well known, the seesaw mechanism describes the tiny neutrino masses by introducing a new high mass scale. In the case of the type-I seesaw model, such a high scale is identical to the right-handed neutrino mass scale. A minimal supersymmetric version of the type-I seesaw model is defined by a superpotential as

$$W_{\text{lepton}} = Y_E^{ij} E_i^c L_j H_1 + Y_N^{ij} N_i^c L_j H_2 + \frac{1}{2} M_N^{ij} N_i^c N_j^c, \tag{1}$$

where N^c, E^c, L, and $H_{1,2}$ are superfields of a singlet neutrino, charged lepton, $SU(2)_L$ lepton doublet, and two Higgs doublets, respectively. The generations are denoted by i and j. Yukawa matrices for charged leptons and neutrinos are defined as Y_E and Y_N, respectively. A Majorana mass matrix is represented as M_N. The soft-supersymmetry-breaking terms in the lepton sector are given by[1]

$$\begin{aligned} -\mathcal{L}_{\text{soft}}^{\text{lepton}} &= (m_L^2)^{ij} \tilde{\ell}_i^\dagger \tilde{\ell}_j + (m_E^2)^{ij} \tilde{e}_i^\dagger \tilde{e}_j + (m_N^2)^{ij} \tilde{\nu}_i^\dagger \tilde{\nu}_j \\ &\quad + (T_E^{ij} \tilde{e}_i^\dagger \tilde{\ell}_j h_1 + T_N^{ij} \tilde{\nu}_i \tilde{\ell}_j h_2 + \text{H.c.}), \end{aligned} \tag{2}$$

where $\tilde{f}$ is a superpartner of f. The quark and gauge sector are defined in the same way as in the minimal supersymmetric standard model (MSSM). We follow the convention and notation defined by SUSY Les Houches Accord 2 [33] in the present paper.

At a low-energy scale where the heavy fields N_i^c are integrated out, the effective higher-dimensional term is given as

$$W_{\text{seesaw}} = \frac{1}{2} K_N^{ij} (L_i H_2)(L_j H_2), \tag{3}$$

$$K_N = -Y_N^T M_N^{-1} Y_N \tag{4}$$

[1]We neglect the term $\tilde{\nu}_i^\dagger \tilde{\nu}_j^\dagger$ [25].

at the tree level. The neutrino mass matrix is obtained from this term after the electroweak symmetry is broken:

$$m_\nu^{ij} = K_N^{ij} v^2 \sin^2\beta, \tag{5}$$

where $v \simeq 174$ GeV, and $\tan\beta$ is the ratio of two vacuum expectation values of the Higgs scalar fields in the superfields H_1 and H_2. Diagonalizing the mass matrix m_ν results in the tiny neutrino masses and the PMNS matrix.

We assume a universality of the soft-SUSY-breaking parameters as

$$(m_L^2)^{ij} = (m_E^2)^{ij} = (m_N^2)^{ij} = M_0^2\delta^{ij}, \qquad T_N^{ij} = M_0 A_0 Y_N^{ij}, \quad T_E^{ij} = M_0 A_0 Y_E^{ij} \tag{6}$$

at the GUT scale μ_G, where M_0 is the universal scalar mass and A_0 is the dimensionless universal trilinear coupling. The soft breaking parameters in the squark and Higgs sector are also taken to be universal. For the gaugino masses, we introduce $M_{1/2}$, assuming the GUT relation. This ansatz clearly implies that the source of LFVs does not exist in the soft-supersymmetry-breaking terms at this scale of the Lagrangian, while it does in the superpotential. For details on these assumptions and references, see Ref. [25].

Below the GUT scale, however, the renormalization group equations (RGEs) of the parameters in Eq. (6) generate a slepton flavor mixing. A main source of the mixing is off-diagonal elements of $(Y_N^\dagger Y_N)^{ij}$. In the approximation that all the singlet neutrinos are decoupled at a scale μ_R, the contribution to the slepton mixing is represented as

$$(m_L^2)^{ij} \simeq -\frac{1}{8\pi^2} M_0^2 (3 + |A_0|^2)(Y_N^\dagger Y_N)^{ij} \ln\frac{\mu_G}{\mu_R}, \tag{7}$$

$$(m_E^2)^{ij} \simeq 0, \tag{8}$$

$$(T_E)^{ij} \simeq -\frac{1}{8\pi^2} M_0 A_0 \hat{Y}_E^{ii} (Y_N^\dagger Y_N)^{ij} \ln\frac{\mu_G}{\mu_R} \tag{9}$$

for $i \neq j$, where $\hat{Y}_E$ is the real positive matrix obtained by diagonalizing Y_E. To be more precise, we need to take into account the threshold effect, because three right-handed neutrinos decouple at different mass scales. The precise treatment of this threshold effect modifies the calculation of the flavor mixing in the slepton sector. As explained in Sec. III, we evaluate the LFVs by taking these effects.

B. Structure of the neutrino Yukawa matrix

Patterns of LFVs are considerably affected by the structure of matrices Y_N and M_N. Here we summarize the parametrizations of them in our analysis. The superpotential for the lepton sector is given in Eq. (1). We decompose Y_E, Y_N, and M_N in Eq. (1) as

$$Y_E = U_E^{[e]\dagger} \hat{Y}_E U_L^{[e]}, \tag{10}$$

$$Y_N = U_N^{[\nu]\dagger} \hat{Y}_N U_L^{[\nu]}, \tag{11}$$

$$M_N = U_N^{[M]\dagger} \hat{M}_N U_N^{[M]*}, \tag{12}$$

where $\hat{Y}_E$, $\hat{Y}_N$, and $\hat{M}_N$ are real positive diagonal matrices and $U_E^{[e]\dagger}$, $U_N^{[\nu]\dagger}$, $U_N^{[M]\dagger}$, $U_L^{[e]}$, $U_L^{[\nu]}$, and $U_N^{[M]}$ are unitary matrices. We define the rotated fields as $L^{[a]} = U_L^{[a]} L$ (for $a = e, \nu$), $E^{c[e]} = U_E^{[e]*} E^c$, and $N^{c[b]} = U_N^{[b]*} N^c$ (for $b = \nu, M$). The superpotential in Eq. (1) is written in terms of $E^{c[e]}$, $L^{[e]}$, and $N^{c[M]}$ as

$$W_{\text{lepton}} = (W_\nu^T \hat{Y}_N V_\nu)^{ij} N_i^{c[M]} L_j^{[e]} H_2 + \hat{Y}_E^{ii} E_i^{c[e]} L_i^{[e]} H_1 + \frac{1}{2}\hat{M}_N^{ii} N_i^{c[M]} N_i^{c[M]}, \tag{13}$$

where $V_\nu = U_N^{[\nu]} U_L^{[e]\dagger}$ has three angles and one phase similarly to the Cabibbo-Kobayashi-Maskawa (CKM) matrix in the quark sector [34], i.e., V_ν is written as

$$V_\nu = \begin{pmatrix} \bar{c}_{12}\bar{c}_{13} & \bar{s}_{12}\bar{c}_{13} & \bar{s}_{13}e^{-i\bar{\delta}_\nu} \\ -\bar{s}_{12}\bar{c}_{23} - \bar{c}_{12}\bar{s}_{23}\bar{s}_{13}e^{i\bar{\delta}_\nu} & \bar{c}_{12}\bar{c}_{23} - \bar{s}_{12}\bar{s}_{23}\bar{s}_{13}e^{i\delta_\nu} & \bar{s}_{23}\bar{c}_{13} \\ \bar{s}_{12}\bar{s}_{23} - \bar{c}_{12}\bar{c}_{23}\bar{s}_{13}e^{i\bar{\delta}_\nu} & -\bar{c}_{12}\bar{s}_{23} - \bar{s}_{12}\bar{c}_{23}\bar{s}_{13}e^{i\delta_\nu} & \bar{c}_{23}\bar{c}_{13} \end{pmatrix}, \tag{14}$$

where $\bar{c}_{ij} = \cos\bar{\theta}_{ij}$, $\bar{s}_{ij} = \sin\bar{\theta}_{ij}$ with $0 \leq \bar{\theta}_{ij} \leq \pi/2$, and $\bar{\delta}_\nu$ is a Dirac CP-violating phase. The matrix $W_\nu = U_N^{[\nu]\dagger} U_N^{[M]}$ is a special unitary matrix, which has three angles and five phases. Therefore, there are in total 18 free parameters in V_ν, W_ν, $\hat{Y}_N$, and $\hat{M}_N$, which cannot be reduced by redefinition of the fields. We define $Y_N^{[M,e]} = W_\nu^T \hat{Y}_N V_\nu$ and $Y_N^{[\nu,e]} = \hat{Y}_N V_\nu$ for later convenience.

On the other hand, the effective superpotential at the low-energy scale is written as in Eq. (3). We introduce another basis as $L^{[e']} = U_L^{[e']} L$, $E^{c[e']} = U_E^{[e']*} E^c$ for the charged leptons and $L^{[\nu']} = U_L^{[\nu']} L$ for the neutrinos so that Y_E, K_N in Eq. (3) are decomposed as

$$Y_E = U_E^{[e']\dagger} \hat{Y}_E U_L^{[e']}, \qquad K_N = U_L^{[\nu']T} \hat{K}_N U_L^{[\nu']}. \tag{15}$$

In this case, we can write the superpotential as

$$W_{\rm lepton}^{\rm eff} = \hat{Y}_E^{ii} E_i^{c[e']} L_i^{[e']} H_1 + \frac{1}{2}(U_\nu^* \hat{K}_N U_\nu^\dagger)^{ij}(L_i^{[e']} H_2)(L_j^{[e']} H_2), \tag{16}$$

where $U_\nu = U_L^{[e']} U_L^{[\nu']\dagger}$ is the PMNS matrix, which has three angles and three phases, i.e., U_ν is defined as

$$U_\nu = \begin{pmatrix} c_{12}c_{13} & s_{12}c_{13} & s_{13}e^{-i\delta_\nu} \\ -s_{12}c_{23} - c_{12}s_{23}s_{13}e^{i\delta_\nu} & c_{12}c_{23} - s_{12}s_{23}s_{13}e^{i\delta_\nu} & s_{23}c_{13} \\ s_{12}s_{23} - c_{12}c_{23}s_{13}e^{i\delta_\nu} & -c_{12}s_{23} - s_{12}c_{23}s_{13}e^{i\delta_\nu} & c_{23}c_{13} \end{pmatrix} \begin{pmatrix} 1 & & \\ & e^{i\alpha_\nu/2} & \\ & & e^{i\beta_\nu/2} \end{pmatrix}, \tag{17}$$

where $c_{ij} = \cos\theta_{ij}$, $s_{ij} = \sin\theta_{ij}$ with $0 \le \theta_{ij} \le \pi/2$, δ_ν is a Dirac CP-violating phase, and α_ν, β_ν are two Majorana CP-violating phases. Neutrino masses are represented by $\hat{K}_N v^2 \sin^2\beta$. Therefore, 9 of 18 parameters in V_ν, W_ν, $\hat{Y}_N$, and $\hat{M}_N$ are used in order to generate three neutrino masses and the components of the PMNS matrix. In other words, the LFV processes depend also on the remaining nine unfixed parameters. We note that the bases $[e]$ and $[e']$ are related as $L_i^{[e]} = P_L^{ii} L_i^{[e']}$ where P_L^{ii} is a diagonal phase matrix. These two bases are different ($P_L \neq \mathbf{1}$) in general with the phase conventions for V_ν and U_ν in Eqs. (14) and (17), respectively.

There are several choices for parametrizing Y_N and M_N. In this paper, we use the following two parameterizations:

(i) *Parametrization 1:* We take the basis $Y_N^{[M,e']} = Y_N^{[M,e]} P_L = W_\nu^T \hat{Y}_N V_\nu P_L$. In this case, the Majorana mass matrix is diagonal, and the neutrino Yukawa matrix is written as [35]

$$Y_N^{[M,e']} = \sqrt{\hat{M}_N} O_N \sqrt{\hat{K}_N} U_\nu^\dagger, \tag{18}$$

where O_N is a complex orthogonal matrix which is given by

$$O_N = \hat{M}_N^{-1/2} W_\nu^T \hat{Y}_N V_\nu P_L U_\nu \hat{K}_N^{-1/2}. \tag{19}$$

We have three parameters in $\hat{M}_N$ and six parameters in O_N. This parametrization befits a *degenerate* structure of M_N, since we can take $\hat{M}_N$ as input parameters.

(ii) *Parametrization 2:* Another parametrization is to take the basis $Y_N^{[\nu,e']} = Y_N^{[\nu,e]} P_L = \hat{Y}_N V_\nu P_L$. In this basis, the Majorana mass matrix is written as

$$M_N^{[\nu]} = Y_N^{[\nu,e']} (U_\nu \hat{K}_N^{-1} U_\nu^T) Y_N^{[\nu,e']T} = W_\nu^* \hat{M}_N W_\nu^\dagger. \tag{20}$$

The neutrino Yukawa matrix $Y_N^{[\nu,e']}$ contains nine free parameters, and thus they control the contributions to LFVs via $Y_N^\dagger Y_N$ as in Eqs. (7)–(9). As will be explained later, it is convenient to apply this parametrization for a *nondegenerate* structure in M_N.

III. ANALYSIS METHOD

In order to analyze low-energy LFV signals in the supersymmetric seesaw model, it is required to evaluate the running effect on the parameters from the GUT scale ($\mu_{\rm G}$) to the electroweak scale. At the GUT scale, we define the parameters of the soft breaking terms in the context of the minimal supergravity—that is, A_0, M_0, and $M_{1/2}$. The neutrino Yukawa matrix Y_N and the Majorana mass matrix M_N are also defined at the GUT scale. After diagonalizing M_N, we obtain the masses of the right-handed neutrinos at their proper scales. Below the scales of right-handed neutrino masses, the soft breaking parameters are evaluated at the SUSY-breaking and electroweak-symmetry-breaking (EWSB) scale ($\mu_{\rm EWSB}$) by solving the RGEs. Then, the physical mass spectrum and the flavor-mixing matrices of SUSY particles are obtained at the electroweak scale. The detailed setup for the evaluation is summarized below.

A. Neutrino sector

Here we show the setup of the neutrino sector. The neutrino mass matrix m_ν^{ij} obtained at the low-energy scale is decomposed as

$$m_\nu^{ij} = (U_\nu^*)^{ik} m_{\nu_k} (U_\nu^\dagger)^{kj}, \tag{21}$$

where U_ν is the PMNS matrix defined in Eq. (17) and m_{ν_k} is a neutrino mass eigenvalue. Since the two squared mass differences of the neutrinos $\Delta m_{ij}^2 = m_{\nu_i}^2 - m_{\nu_j}^2$ satisfy $|\Delta m_{32}^2| \gg |\Delta m_{21}^2|$, the neutrino mass spectra can be hierarchical. The cases for $m_{\nu_3} \gg m_{\nu_2} > m_{\nu_1}$ and $m_{\nu_2} > m_{\nu_1} \gg m_{\nu_3}$ are referred to as normal and inverted hierarchies, respectively. In our analysis, we consider both cases.

B. Renormalization group equations

We solve the RGEs of the SUSY parameters including the seesaw sector by using the public code SPheno 3.2.4 written by W. Porod and F. Staub [36]. Two-loop running effects and complete one-loop corrections to all SUSY and Higgs particle masses are included as explained in

Ref. [36]. As for the Higgs boson, its pole mass is calculated at the two-loop level. The setup in our study is listed as follows:

(i) The GUT scale is set to be $\mu_{\rm G} = 2 \times 10^{16}$ GeV.
(ii) The EWSB scale is determined at $\mu_{\rm EWSB} = \sqrt{m_{\tilde{t}_1} m_{\tilde{t}_2}}$, where $m_{\tilde{t}_{1,2}}$ are stop masses.
(iii) The neutrino Yukawa matrix with a specific structure is defined at the GUT scale.
(iv) The Higgsino mass parameter μ and A_0 are assumed to be real to avoid constraints from experimental searches for various electric dipole moments [37].

We take into account the threshold effect mentioned in Sec. II A by integrating out right-handed neutrinos one by one at their proper scales. This effect generates contributions to the slepton mixing in addition to those given in Eqs. (7)–(9). Furthermore, the seesaw relation shown in Eq. (4) is modified [38,39].

Among 18 parameters in Y_N and M_N, we choose nine of them as inputs at the GUT scale and adjust the others to reproduce the neutrino masses m_{ν_i} and the PMNS matrix U_ν. To do that, we define $m_{\nu_i}^{\rm G}$ and $U_\nu^{\rm G}$ at the GUT scale as

$$(U_\nu^{\rm G*})^{ik} m_{\nu_k}^{\rm G} (U_\nu^{\rm G\dagger})^{kj} = -v^2 \sin^2\beta (Y_N^T M_N^{-1} Y_N)^{ij}. \quad (22)$$

We numerically determine $U_\nu^{\rm G}$ and $m_\nu^{\rm G}$, which reproduce the PMNS matrix and the neutrino masses at the low-energy scale by an iterative method. We note that $s_{12}^{\rm G}$, $\Delta m_{32}^{2,\rm G}$, and $\Delta m_{21}^{2,\rm G}$ in Eq. (22) are sensitive to the running effect compared with the other components [38,39].

C. Structure of Y_N

In the present work, we investigate LFV signals in two cases with specific structures in Y_N and M_N: the *degenerate case* and the *nondegenerate case*. For each case, we apply the appropriate parametrization, which we have shown in the previous section.

Degenerate case: First, we consider the degenerate case (D case), which means that the Majorana mass matrix is assumed to be proportional to the unit matrix. In this case, we apply parametrization 1. We decompose the matrix O_N as

$$O_N = \tilde{O}_N e^{iA_N}, \qquad A_N = \begin{pmatrix} 0 & a & b \\ -a & 0 & c \\ -b & -c & 0 \end{pmatrix}, \quad (23)$$

where $\tilde{O}_N$ is a real orthogonal matrix and A_N is a real antisymmetric matrix $A_N^T = -A_N$. The matrix $\tilde{O}_N$ is irrelevant for the LFV signals, since the source of the flavor mixing comes from $Y_N^\dagger Y_N$. Thus, we take $\tilde{O}_N = \mathbf{1}$ without loss of generalities. The neutrino Yukawa matrix Y_N is written as

$$Y_N = \frac{\sqrt{\tilde{M}_N}}{v \sin\beta} e^{iA_N} \begin{pmatrix} \sqrt{m_{\nu_1}} & & \\ & \sqrt{m_{\nu_2}} & \\ & & \sqrt{m_{\nu_3}} \end{pmatrix} U_\nu^\dagger, \quad (24)$$

where $\tilde{M}_N$ is the degenerate Majorana mass eigenvalue. As for the parameters in A_N, we take $a = b = 0$ ($b = c = 0$) for the normal (inverted) hierarchical mass spectrum of the neutrinos, since the contributions of a and b (b and c) are subdominant according to the analysis in Ref. [26]. This can be understood as follows: If we expand the off-diagonal element $(Y_N^\dagger Y_N)_{ij}$ by a, b, and c assuming $|a|, |b|, |c| \ll 1$, the contributions of a, b, and c appear at the leading order in the combinations of $|a|\sqrt{m_{\nu_1} m_{\nu_2}}$, $|b|\sqrt{m_{\nu_1} m_{\nu_3}}$, and $|c|\sqrt{m_{\nu_2} m_{\nu_3}}$. In the case of the normal hierarchy, the contributions of $|a|\sqrt{m_{\nu_1} m_{\nu_2}}$ and $|b|\sqrt{m_{\nu_1} m_{\nu_3}}$ are not significant compared with $|c|\sqrt{m_{\nu_2} m_{\nu_3}}$. For example, the element $(Y_N^\dagger Y_N)_{12}$ which induces $\mu \to e\gamma$ can be represented as

$$\begin{aligned}(Y_N^\dagger Y_N)_{12} \simeq \frac{\tilde{M}_N}{v^2 \sin^2\beta} \big(& (m_{\nu_2} - m_{\nu_1}) c_{12} s_{12} c_{23} \\ & + (m_{\nu_3} - m_{\nu_2}) s_{13} s_{23} e^{-i\delta_\nu} \\ & + 2ic \sqrt{m_{\nu_2} m_{\nu_3}} s_{12} s_{23} e^{i(\alpha_\nu - \beta_\nu)} \big) \end{aligned} \quad (25)$$

with this approximation. The expression for the inverted hierarchy is obtained in a similar way.

Nondegenerate case: Second, we consider the nondegenerate case (ND case) for the structure of M_N. In this case, we apply parametrization 2, and $Y_N^\dagger Y_N$ can be considered as an input. Thus, the Majorana mass matrix M_N is determined by Eq. (20). To see how large $\mathcal{B}(\tau \to \mu\gamma)$ can be within the constraint on $\mathcal{B}(\mu \to e\gamma)$, we take $\bar{\theta}_{12} = \bar{\theta}_{13} = 0$. Accordingly, Y_N is parametrized as

$$Y_N = \begin{pmatrix} y_1 & & \\ & y_2 & \\ & & y_3 \end{pmatrix} \begin{pmatrix} 1 & 0 & 0 \\ 0 & \cos\theta & \sin\theta \\ 0 & -\sin\theta & \cos\theta \end{pmatrix} P_L, \quad (26)$$

where $\theta = \bar{\theta}_{23}$. We also take $P_L = \mathbf{1}$ for simplicity and consider $y_1, y_2, y_3 \lesssim O(1)$. Even though $\mu \to e\gamma$ and $\tau \to e\gamma$ do not occur in the approximation using Eqs. (7)–(9), the threshold effects generate nonzero contributions to $\mu \to e\gamma$ and $\tau \to e\gamma$. In the case of $\bar{\theta}_{12} = \bar{\theta}_{23} = 0$, a similar consideration can be applied for $\tau \to e\gamma$.

D. Observables

In this subsection, we summarize the formulas of relevant processes. The LFV process emitting a photon, $\ell_j \to \ell_i \gamma$, is generated by the $\mathcal{O}_7$ operator, which is defined as

$$\mathcal{L}_{\rm eff}^{\ell\to\ell'\gamma} = C_{7L}^{ij}O_{7L}^{ij} + C_{7R}^{ij}O_{7R}^{ij} + \text{H.c.}, \tag{27}$$

$$\mathcal{O}_{7_R^L}^{ij} = F_{\mu\nu}\bar{\ell}_i\sigma^{\mu\nu}\left(\frac{1\mp\gamma^5}{2}\right)\ell_j, \tag{28}$$

where $\sigma^{\mu\nu} = (i/2)[\gamma^\mu, \gamma^\nu]$ and the coefficients $C_{7L,7R}^{ij}$ are obtained from contributions via lepton-flavor-mixing loop diagrams. Then, the decay rate is given by

$$\Gamma(\ell_j \to \ell_i\gamma) = \frac{m_{\ell_j}^3}{4\pi}(|C_{7L}^{ij}|^2 + |C_{7R}^{ij}|^2), \tag{29}$$

where we neglect the lepton mass in the final state. In the SM, neutrino mixings contribute to C_{7R}^{ij} with a strong suppression factor as $\Delta m_{ij}^2/m_W^2$. In a supersymmetric model, since sleptons and sneutrinos also carry flavor indices, loop diagrams with sleptons or sneutrinos affect $\ell_j \to \ell_i\gamma$. The coefficients $C_{7L,7R}^{ij}$ are written in terms of masses and flavor-mixing matrices of SUSY particles [40,41].

For the quark sector, extra flavor mixings exist in a supersymmetric model. Even if the squark mass matrix is assumed to be diagonal at the GUT scale, off-diagonal elements are generated by the RGE. The off-diagonal elements induce the SUSY contributions to flavor-changing observables via loop diagrams in the quark sector. Among them, $b \to s$ transition processes such as $B \to X_s\gamma$ and $B_s \to \ell^+\ell^-$ are important. The effective Lagrangians for these processes are given by

$$\mathcal{L}_{\rm eff}^{B_s\to\ell^+\ell^-} = \frac{\alpha G_F}{\sqrt{2}\pi\sin^2\theta_W}V_{ts}^*V_{tb}\sum_{i=A,S,P}(C_i\mathcal{O}_i + C_i'\mathcal{O}_i') + \text{H.c.}, \tag{30}$$

$$\mathcal{O}_A = (\bar{s}_L\gamma_\mu b_L)(\bar{\ell}\gamma^\mu\gamma_5\ell), \qquad \mathcal{O}_A' = (\bar{s}_R\gamma_\mu b_R)(\bar{\ell}\gamma^\mu\gamma_5\ell), \tag{31}$$

$$\mathcal{O}_S = m_b(\bar{s}_R b_L)(\bar{\ell}\ell), \qquad \mathcal{O}_S' = m_s(\bar{s}_L b_R)(\bar{\ell}\ell), \tag{32}$$

$$\mathcal{O}_P = m_b(\bar{s}_R b_L)(\bar{\ell}\gamma^5\ell), \qquad \mathcal{O}_P' = m_s(\bar{s}_L b_R)(\bar{\ell}\gamma^5\ell), \tag{33}$$

and

$$\mathcal{L}_{\rm eff}^{B\to X_s\gamma} = 2\sqrt{2}G_F V_{ts}^*V_{tb}\sum_{i=7,8}(C_i\mathcal{O}_i + C_i'\mathcal{O}_i') + \text{H.c.}, \tag{34}$$

$$\mathcal{O}_7 = \frac{e}{16\pi^2}m_b\bar{s}_L\sigma^{\mu\nu}b_R F_{\mu\nu}, \qquad \mathcal{O}_7' = \frac{e}{16\pi^2}m_s\bar{s}_R\sigma^{\mu\nu}b_L F_{\mu\nu}, \tag{35}$$

$$\mathcal{O}_8 = \frac{g_s}{16\pi^2}m_b\bar{s}_L\sigma^{\mu\nu}T^a b_R G_{\mu\nu}^a, \qquad \mathcal{O}_8' = \frac{g_s}{16\pi^2}m_s\bar{s}_R\sigma^{\mu\nu}T^a b_L G_{\mu\nu}^a. \tag{36}$$

The contributions of SUSY particles are all included in the Wilson coefficients $C_i^{(\prime)}$. The analytical formulas for $\mathcal{B}(B_s \to \ell^+\ell^-)$ and $\mathcal{B}(B \to X_s\gamma)$ are found in Refs. [42] and [43], respectively.

In the supersymmetric model, the Higgs boson mass is less than the Z boson mass at the tree level and increases owing to a radiative correction [44]. The Higgs boson mass is evaluated including two-loop corrections following the formula in Ref. [45], which is implemented in SPheno.

IV. NUMERICAL RESULT

In this section, we present the allowed region of the SUSY parameter space and predictions on the patterns of the LFV signals.

A. Inputs and constraints

For the neutrino parameters, we adjust the parameters at the GUT scale so that the mass differences and mixings are consistent with the present neutrino oscillation data [16]. To do that, we apply the allowed range for the neutrino parameters at the low-energy scale shown in Table I. In our calculation, we take the lightest neutrino mass to be $m_{\nu_{1(3)}} = 0.0029$–0.0031 eV in the normal (inverted) hierarchy. We emphasize that the angle θ_{13} has been precisely determined by experiments and found to be not zero [17–21]. By the combination of the reactor experiments

TABLE I. Experimental results and allowed ranges for the neutrino parameters which we take into account in our numerical calculation. The experimental values are results from the fitted analysis assuming the normal (inverted) hierarchy of neutrino masses. We apply the same allowed ranges for both the normal and inverted hierarchical cases.

Measurement	Experimental result [16]	Allowed range
$\Delta m_{21}^2 \times 10^5$ eV^{-2}	$7.54^{+0.26}_{-0.22}(7.54^{+0.26}_{-0.22})$	7.3–7.8
$\lvert\Delta m_{32}^2\rvert \times 10^3$ eV^{-2}	$2.39 \pm 0.06(2.42 \pm 0.06)$	2.3–2.5
$\sin^2\theta_{12}$	$0.308 \pm 0.017(0.308 \pm 0.017)$	0.29–0.33
$\sin^2\theta_{23}$	$0.437^{+0.033}_{-0.023}(0.455^{+0.039}_{-0.031})$	0.41–0.49
$\sin^2\theta_{13}$	$0.0234^{+0.0020}_{-0.0019}(0.0240^{+0.0019}_{-0.0022})$	0.022–0.026

TABLE II. Experimental results on flavor signals and masses and their allowed ranges taken in our analysis.

Measurement	Experimental result	Allowed range
m_h	ATLAS: $(125.36 \pm 0.37 \pm 0.18)$ GeV [6] CMS: $(125.03^{+0.26}_{-0.27})$ GeV [7]	(126 ± 2) GeV
$\mathcal{B}(\bar{B} \to X_s\gamma) \times 10^4$	$3.43 \pm 0.21 \pm 0.07$ [10]	3.43 ± 0.62
$\mathcal{B}(B_s \to \mu^+\mu^-) \times 10^9$	2.9 ± 0.7 [12]	2.9 ± 0.7
$\mathcal{B}(\mu \to e\gamma) \times 10^{13}$	< 5.7 [22]	< 5.7
$\mathcal{B}(\tau \to \mu(e)\gamma) \times 10^8$	$< 4.4(3.3)$ [23]	$< 4.4(3.3)$
$M_{\tilde{g}}$	> 1.4 TeV [8,9]	> 1.4 TeV
$M_{\tilde{q}}$	> 1.7 TeV [8,9]	> 1.7 TeV

and the experiment of electron neutrino appearance from a muon neutrino beam in Refs. [46,47], a preferred range of δ_ν can be obtained, but the constraint is not strong. As for the Majorana CP-violating phases, there is no experimental constraint. In our analysis, we treat the CP-violating phases as free parameters.

Recent results in LHC experiments put constraints on the SUSY parameter space. First, the Higgs boson mass is measured as $m_h \simeq 126$ GeV [6,7]. For the MSSM, this value implies a heavy stop or a large left-right mixing in the stop sector. Second, direct searches for the squarks and the gluino impose the constraints on their masses [8,9]. The lower limit of the gluino mass is around 1.4 TeV, and that of the squark masses for the first and second generations is about 1.7 TeV.

Flavor experiments have also improved their results over the past few years. It is known that the branching ratio of $\bar{B} \to X_s\gamma$ put a severe constraint on the SUSY parameter space. Including the recent updated result of the *BABAR* experiment [48], the latest world average of the branching ratio is $\mathcal{B}(\bar{B} \to X_s\gamma) = (3.43 \pm 0.21 \pm 0.07) \times 10^{-4}$ [10]. Another important process is $B_s \to \mu^+\mu^-$, which was first observed by the LHCb Collaboration [11]. The latest result is $\mathcal{B}(B_s \to \mu^+\mu^-) = (2.9 \pm 0.7) \times 10^{-9}$ [12], combining the results obtained by the LHCb [13] and CMS [14] collaborations.

For LFV processes, an improved constraint on $\mu \to e\gamma$ is obtained as $\mathcal{B}(\mu \to e\gamma) < 5.7 \times 10^{-13}$ at a 90% confidence level (C.L.) by the MEG Collaboration [22]. The flavor-violating decays of the tau lepton, $\tau \to \mu\gamma$ and $\tau \to e\gamma$, are also constrained by the *BABAR* [23] and Belle [24] collaborations. The recent bounds on the branching ratios are $\mathcal{B}(\tau \to \mu\gamma) < 4.4 \times 10^{-8}$ and $\mathcal{B}(\tau \to e\gamma) < 3.3 \times 10^{-8}$.

In order to take these constraints into account, we apply the allowed ranges as listed in Table II. For the allowed range of $\mathcal{B}(\bar{B} \to X_s\gamma)$, we include theoretical uncertainty [49] and experimental uncertainties within 2σ ranges. In order to take the theoretical uncertainties of the Higgs boson mass into account, we assign ± 2 GeV for the allowed range as shown in Table II. We take into account the only experimental error in $\mathcal{B}(B_s \to \mu^+\mu^-)$. As for the SUSY particle mass bounds, the quoted bounds are used to constrain the SUSY parameter space in our analysis, even though these bounds are obtained under some assumption for the SUSY spectrum.

In Figs. 1 and 2, we show the excluded region plots for the $(M_0, M_{1/2})$ plane by taking into account the constraints discussed above. In the figures, colored regions are excluded and the white regions are allowed. We take the normal hierarchy for neutrino masses, and the CP-violating phases in the PMNS matrix are assumed as $\delta_\nu = \alpha_\nu = \beta_\nu = 0$. For the neutrino Yukawa matrix Y_N, we consider the degenerate and the nondegenerate cases in Figs. 1 and 2, respectively. For the degenerate case, we take $\tilde{M}_N = 7 \times 10^{12}$ GeV and $O_N = \mathbf{1}$. For the nondegenerate case, we take $y_1 = 0.05$, $y_2 = y_3 = 1.5$, and $\theta = \pi/4$. As for the SUSY parameters, $\mathrm{sign}(\mu)$, A_0, and $\tan\beta$ are fixed as shown in the figures. In the yellow region, the lightest SUSY particle (LSP) is a charged particle. In the black region in Fig. 1(a), the EWSB does not occur. The black dotted lines show the contours of the Higgs boson mass for $m_h = 124$, 126, and 128 GeV, and the gray region shows that the Higgs boson mass is outside of the allowed range. The blue and green regions are excluded by the lower-mass bounds of the squark and gluino, respectively. The magenta, orange, and cyan regions are not allowed by the experimental data of $\mathcal{B}(\bar{B} \to X_s\gamma)$, $\mathcal{B}(B_s \to \mu^+\mu^-)$, and $\mathcal{B}(\mu \to e\gamma)$, respectively. We also show the contours of $\mathcal{B}(\mu \to e\gamma)$ and $\mathcal{B}(\tau \to \mu\gamma)$ with the cyan solid and red dashed lines, respectively. As is well known, the allowed region from the Higgs boson mass depends on A_0, since the left-right mixing in the stop sector affects the Higgs boson mass. One can see that the squark and slepton masses are large for $A_0 = 0$, and their masses are relatively small for $A_0 = -2$. Moreover, the lepton flavor mixing is enhanced for $A_0 = -2$. Thus, the LFV decay rates are larger for $A_0 = -2$ than those for $A_0 = 0$. It can be seen from Figs. 1 and 2 in the same setup for $[\mathrm{sign}(\mu), A_0, \tan\beta]$ that the Higgs boson mass is also affected by the structure in Y_N. This is because Y_N alters the renormalization group running of the stop A term and the stop masses. The constraints from the B physics are also important. In a certain parameter region, only $\mathcal{B}(\bar{B} \to X_s\gamma)$ gives a constraint. In Fig. 1, only $\mathcal{B}(\mu \to e\gamma)$ can be large in the allowed region, whereas both

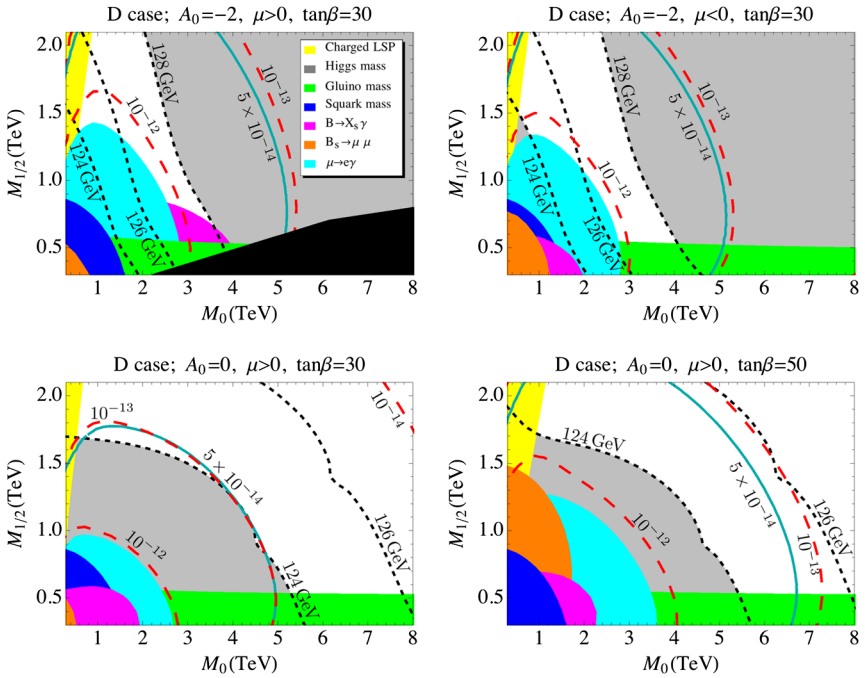

FIG. 1 (color online). Excluded region plots for $(M_0, M_{1/2})$ with fixed parameters of $[\mathrm{sign}(\mu), A_0, \tan\beta]$ in the degenerate case with the normal hierarchical neutrino masses. The parameters in the neutrino sector are assumed as $\tilde{M}_N = 7\times10^{12}$ GeV and $O_N = \mathbf{1}$. Each colored region is excluded by the observable as exhibited in the legend. The dotted, dashed, and solid lines show the contours of m_h, $\mathcal{B}(\tau\to\mu\gamma)$, and $\mathcal{B}(\mu\to e\gamma)$, respectively.

$\mathcal{B}(\mu\to e\gamma)$ and $\mathcal{B}(\tau\to\mu\gamma)$ could be close to the current experimental upper bounds in the case of Fig. 2. We note that our result is consistent with the other recent studies in Refs. [29,30].

It is pointed out that there is around 3σ deviation of the muon $g-2$ between the SM prediction and the present experimental result [50,51]. In the context of the minimal supergravity, it is known that the SUSY contribution to the

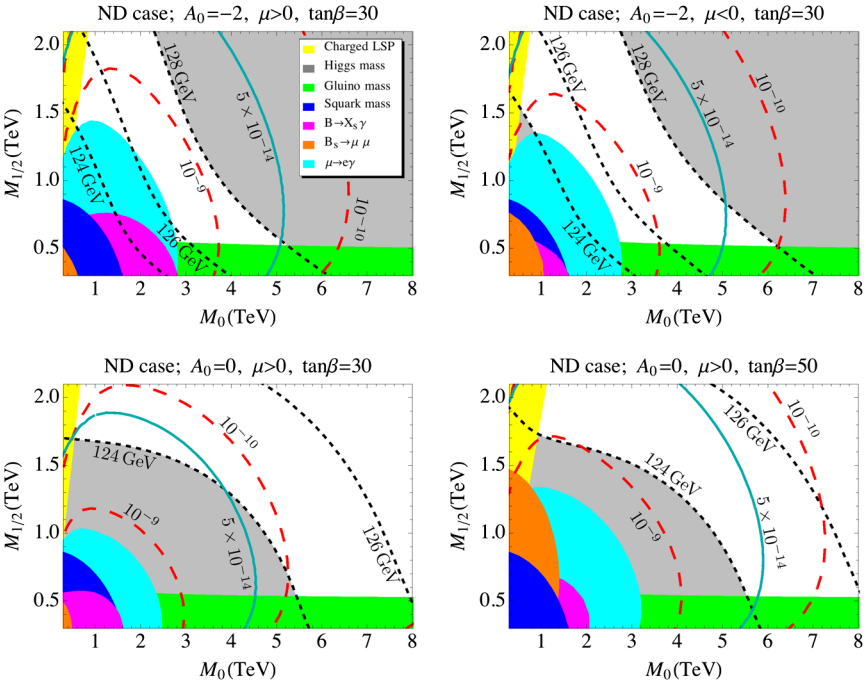

FIG. 2 (color online). Excluded region plots in the nondegenerate case with the normal hierarchical neutrino masses. The parameters in Y_N are assumed as $y_1 = 0.05$, $y_2 = y_3 = 1.5$, and $\theta = \pi/4$. The notation is the same as in Fig. 1.

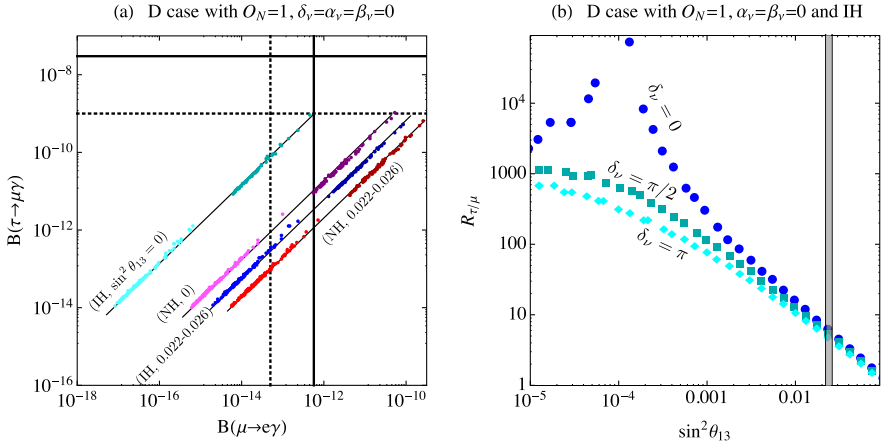

FIG. 3 (color online). (a) Correlation between $\mathcal{B}(\mu \to e\gamma)$ and $\mathcal{B}(\tau \to \mu\gamma)$ in the degenerate case with $O_N = \mathbf{1}$. The SUSY parameters $(M_{1/2}, M_0, A_0)$ are randomly generated, and we take $\tan\beta = 30$ and $\mu > 0$. The upper-right group of dots along each line corresponds to $\tilde{M}_N = 5 \times 10^{14}$ GeV, and the lower-left one corresponds to $\tilde{M}_N = 7 \times 10^{12}$ GeV. The results of NH and IH within $\sin^2\theta_{13} = 0.022$–$0.026$ and with $\sin^2\theta_{13} = 0$ are shown as indicated. The vertical and horizontal solid lines show the present upper bounds of $\mathcal{B}(\mu \to e\gamma)$ and $\mathcal{B}(\tau \to \mu\gamma)$, respectively. The dotted lines indicate expected sensitivities at SuperKEKB/Belle II and MEG II. (b) The ratio $R_{\tau/\mu} = \mathcal{B}(\tau \to \mu\gamma)/\mathcal{B}(\mu \to e\gamma)$ for IH as a function of $\sin^2\theta_{13}$. The gray region is the present experimental value of $\sin^2\theta_{13}$.

muon $g-2$ is too small to explain the deviation within the other constraints. In fact, in the allowed regions in Figs. 1 and 2, the contribution is suppressed. However, both theoretical and experimental uncertainties are still significant, and therefore the deviation is not conclusive. Thus, in this study, we do not use the muon $g-2$ as a constraint.[2]

The μ-e conversions in nuclei are also important processes to search for evidence of the LFV. In the type-I SUSY seesaw model where the photon dipole operator gives dominant contributions,[3] the rate of μ-e conversion and $\mu \to e\gamma$ is estimated, for example, as $\mathcal{B}(\mu^- \mathrm{Al} \to e^- \mathrm{Al})/\mathcal{B}(\mu \to e\gamma) \simeq 0.0026$ [53]. Thus, we can easily translate the constraint and prediction for $\mu \to e\gamma$ into those for μ-e conversion. Taking into account the present upper bound on the μ-e conversion [54], the constraint from the $\mu \to e\gamma$ experiment is more important.

B. LFV signals

We investigate signals of LFV for the degenerate case and the nondegenerate case in the neutrino sector.[4] In particular, we discuss the correlation between $\mathcal{B}(\mu \to e\gamma)$ and $\mathcal{B}(\tau \to \mu\gamma)$.

1. Degenerate case

In Ref. [25], it has been found that $\mathcal{B}(\mu \to e\gamma)$ and $\mathcal{B}(\tau \to e\gamma)$ can be suppressed while keeping a large $\mathcal{B}(\tau \to \mu\gamma)$ in the simplest degenerate case with $O_N = \mathbf{1}$ in Eq. (24), if θ_{13} is chosen to be zero and neutrino masses are inversely hierarchical. This is because the off-diagonal elements of $Y_N^\dagger Y_N$ are approximately written as

$$(Y_N^\dagger Y_N)_{12,13} \propto \frac{\tilde{M}_N}{v^2} \cdot \frac{\Delta m_{21}^2}{m_{\nu_1} + m_{\nu_2}},$$
$$(Y_N^\dagger Y_N)_{23} \propto \frac{\tilde{M}_N}{v^2} \cdot \frac{\Delta m_{32}^2}{m_{\nu_2} + m_{\nu_3}} \tag{37}$$

for $\theta_{13} = 0$ in the PMNS matrix. Thus, $\mathcal{B}(\mu \to e\gamma)$ and $\mathcal{B}(\tau \to e\gamma)$ are strongly suppressed for the inverted hierarchical case.

Taking into account recent experimental results from neutrino experiments, we show the correlation between $\mathcal{B}(\mu \to e\gamma)$ and $\mathcal{B}(\tau \to \mu\gamma)$ in the simplest degenerate case within $\sin^2\theta_{13} = 0.022$–$0.026$ in Fig. 3(a). We also present the result with $\sin^2\theta_{13} = 0$ for comparison. We take $\delta_\nu = \alpha_\nu = \beta_\nu = 0$ for both the NH and IH cases. As for the SUSY inputs, we randomly vary them within

$$0 < M_0 < 8 \text{ TeV}, \qquad 0 < M_{1/2} < 2 \text{ TeV},$$
$$-2 < A_0 < 2, \tag{38}$$

taking the others as $\mu > 0$, $\tan\beta = 30$. The upper-right group of dots along each line corresponds to the Majorana mass $\tilde{M}_N = 5 \times 10^{14}$ GeV, and the lower-left one

[2]There are several models where the deviation is explained in the SUSY model beyond the context of the minimal supergravity by splitting the mass spectrum of colored SUSY particles and that of sleptons, see e.g., Ref. [52].

[3]Notice that in the case of large $\tan\beta$ and small mass of the CP-odd Higgs boson, the Higgs mediated loop contributions become significant and thus must be taken into account, see e.g., Ref. [53]. In the allowed regions in Figs. 1 and 2, such contributions are small.

[4]The Higgs boson decay into a lepton-flavor-violating final state such as $h \to \tau\mu$ is also one of the interesting processes. A recent experimental study is given in Ref. [55]. In the type-I SUSY seesaw model, its branching ratio is enhanced compared with one in the non-SUSY seesaw model, but it does not exceed $\sim 10^{-14}$ in the degenerate case [56].

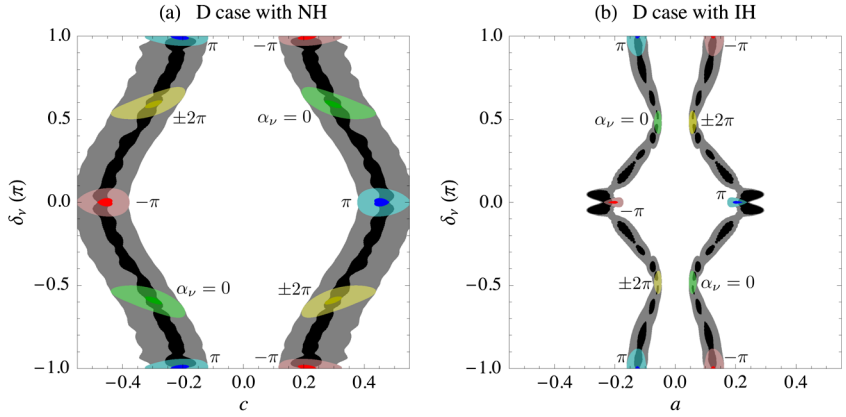

FIG. 4 (color online). Contour plots of $R_{\tau/\mu}$ on the planes of (c, δ_ν) and (a, δ_ν) for (a) normal and (b) inverted hierarchical cases. The black (gray) region corresponds to $R_{\tau/\mu} > 1800$ (100). The regions of $R_{\tau/\mu} > 1800$ (100) with the Majorana CP-violating phases being fixed as $\beta_\nu = 0$, $\alpha_\nu = 0$, $\pm\pi$, and $\pm 2\pi$ are also shown with darker (lighter) color.

corresponds to $\tilde{M}_N = 7 \times 10^{12}$ GeV. We plot points allowed by the constraints listed in Table II except for $\mathcal{B}(\mu \to e\gamma)$ and $\mathcal{B}(\tau \to \mu\gamma)$. The vertical and horizontal solid lines represent the present experimental upper limits on $\mathcal{B}(\mu \to e\gamma)$ and $\mathcal{B}(\tau \to \mu\gamma)$, respectively. We also show the possible reaches of $\mathcal{B}(\tau \to \mu\gamma) \simeq 10^{-9}$ expected at SuperKEKB/Belle II and $\mathcal{B}(\mu \to e\gamma) \simeq 5 \times 10^{-14}$ at MEG II [32] with dotted lines. We find that the ratio $R_{\tau/\mu} = \mathcal{B}(\tau \to \mu\gamma)/\mathcal{B}(\mu \to e\gamma)$ is insensitive to $\tilde{M}_N$ and the SUSY parameters, whereas it is sensitive to θ_{13} and the mass ordering. We also show $R_{\tau/\mu}$ as a function of $\sin^2\theta_{13}$ for the inverted hierarchical cases with $\delta_\nu = 0$, $\pi/2$, and π in Fig. 3(b). Although $R_{\tau/\mu}$ is enhanced by several orders of magnitude if $\sin^2\theta_{13} \sim 10^{-4}$, such an enhancement does not occur for the present value of $\sin^2\theta_{13}$.

The signals of LFV depend on the phase parameters δ_ν, α_ν, and β_ν in the PMNS matrix and a, b, and c defined in Eq. (23). In the normal hierarchical case, the Majorana CP-violating phase contribution always appears in the form of $\alpha_\nu - \beta_\nu$ because $m_{\nu_1} \ll m_{\nu_2}$. As explained in the Sec. III C, the contribution of a and b is negligible. Therefore, we take $\beta_\nu = a = b = 0$. Similarly, in the inverted hierarchical case, we take $\beta_\nu = b = c = 0$. In Fig. 4, the region in which the maximal value of $R_{\tau/\mu}$ in the range $-2\pi \le \alpha_\nu \le 2\pi$ is larger than 1800 (100) is shown in dark (light) gray. The value $R_{\tau/\mu} > 1800$ means $\mathcal{B}(\tau \to \mu\gamma) > 10^{-9}$ for $\mathcal{B}(\mu \to e\gamma) = 5.7 \times 10^{-13}$, the current experimental bound. When we fix the Majorana CP-violating phases as $\alpha_\nu = 0$, $\pm\pi$, and $\pm 2\pi$, the regions are limited as exhibited in the figures. The horizontal width of the gray region in Fig. 4(a) is proportional to $1/\sqrt{m_{\nu_2} m_{\nu_3}}$, and that in Fig. 4(b) to $1/\sqrt{m_{\nu_1} m_{\nu_2}}$. This explains the smaller region of enhancement in the IH case [Fig. 4(b)]. From this analysis, we conclude that there still remain possibilities to obtain $\mathcal{B}(\tau \to \mu\gamma) > 10^{-9}$ in the degenerate case with the CP-violating parameters of c (or a), δ_ν and α_ν.

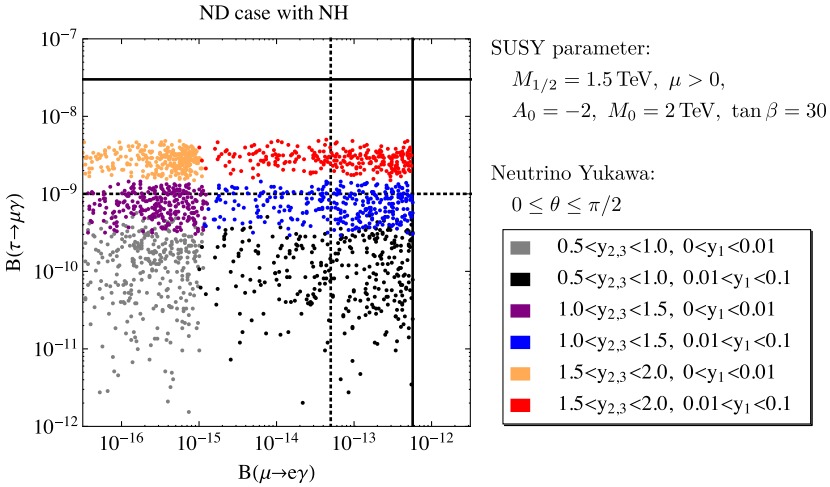

FIG. 5 (color online). Correlation between $\mathcal{B}(\mu \to e\gamma)$ and $\mathcal{B}(\tau \to \mu\gamma)$ in the nondegenerate case. The parameters (y_1, y_2, y_3, θ) in the Y_N are randomly generated within the designated range, and the SUSY parameters are fixed as $M_{1/2} = 1.5$ TeV, $M_0 = 2.0$ TeV, $A_0 = -2$, $\tan\beta = 30$, and $\mu > 0$. The solid lines show the present upper bounds of $\mathcal{B}(\mu \to e\gamma)$ and $\mathcal{B}(\tau \to \mu\gamma)$. The dotted lines indicate expected sensitivities at SuperKEKB/Belle II and MEG II.

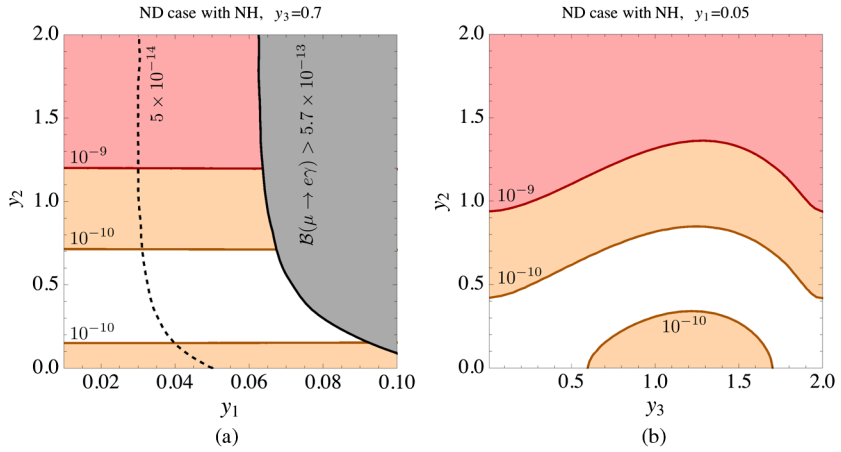

FIG. 6 (color online). Contour plots of $\mathcal{B}(\tau\to\mu\gamma)$ on planes of parameters in the neutrino Yukawa matrix in the nondegenerate case with the normal hierarchy and $\theta=\pi/4$. The red (orange) lines are $\mathcal{B}(\tau\to\mu\gamma)=10^{-9}$ (10^{-10}). The gray region is excluded by the present bound of $\mathcal{B}(\mu\to e\gamma)$. The dotted line shows the expected sensitivity of MEG II, $\mathcal{B}(\mu\to e\gamma)=5\times10^{-14}$.

There are several experimental studies on δ_ν by the T2K [47], MINOS [46], and Super Kamiokande [57] collaborations. For example, the T2K Collaboration has reported that the Dirac CP-violating phase of $0.19\pi<\delta_\nu<0.8\pi(-0.04\pi<\delta_\nu<\pi)$ is excluded at a 90% C.L. for the normal (inverted) hierarchy combining their result with measurements of $\sin^2\theta_{13}$ from reactor experiments.

2. Nondegenerate case

We investigate $\mu\to e\gamma$ and $\tau\to\mu\gamma$ in the nondegenerate case. In order to simplify the following analysis, we assume the normal hierarchy for the neutrino masses and no CP-violating phases in the lepton sector, namely $\delta_\nu=\alpha_\nu=\beta_\nu=0$. As explained in the previous section, we apply the parametrization in Eq. (26) to this case. In Fig. 5, we show a scatter plot that represents the correlation between $\mathcal{B}(\tau\to\mu\gamma)$ and $\mathcal{B}(\mu\to e\gamma)$. In this plot, we explore the parameter space of (y_1,y_2,y_3,θ) in Y_N, fixing SUSY parameters as $M_{1/2}=1.5$ TeV, $M_0=2.0$ TeV, $A_0=-2$, $\tan\beta=30$, and $\mu>0$. These parameters satisfy the constraints in Table II. For the parameters y_1, y_2, and y_3, we divide their regions as indicated in the figure to show the dependence on them. The mixing angle between the second and third generations is taken in the region $0\le\theta\le\pi/2$. It can be seen that $\mathcal{B}(\mu\to e\gamma)$ is sensitive to y_1 and $\mathcal{B}(\tau\to\mu\gamma)$ depends on y_2 and y_3. Large values of y_2 and y_3 are required for the enhancement of $\mathcal{B}(\tau\to\mu\gamma)$. The branching ratios for both tau and muon LFV decays can be large enough to be observed in the near future.

In order to see this situation more clearly, we show the contour plots of $\mathcal{B}(\tau\to\mu\gamma)$ on planes of (y_1,y_2) in Fig. 6(a) and (y_3,y_2) in Fig. 6(b) with $\theta=\pi/4$. We take $y_3=0.7$ in Fig. 6(a) and $y_1=0.05$ in Fig. 6(b). In the red (orange) regions, $\mathcal{B}(\tau\to\mu\gamma)$ is larger than 10^{-9} (10^{-10}). We also show $\mathcal{B}(\mu\to e\gamma)$ in Fig. 6(a). The gray region is excluded by the current experimental upper bound of $\mathcal{B}(\mu\to e\gamma)$. In the whole region in Fig. 6(b), $\mathcal{B}(\mu\to e\gamma)\simeq3\times10^{-13}$. As

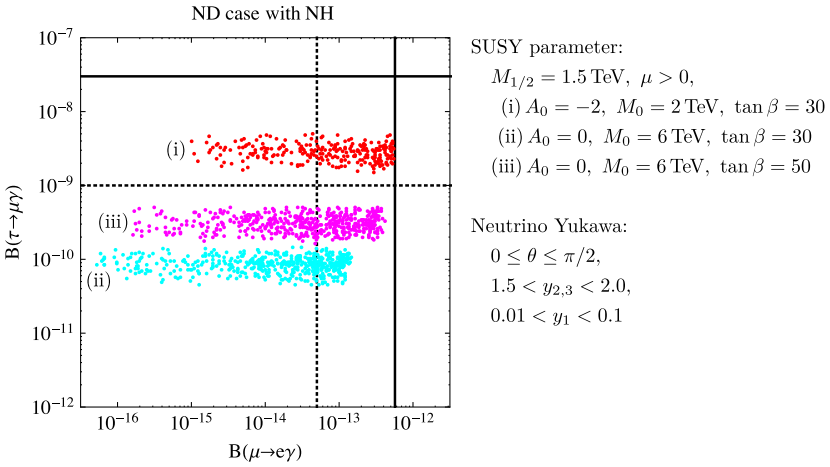

FIG. 7 (color online). Correlation between $\mathcal{B}(\mu\to e\gamma)$ and $\mathcal{B}(\tau\to\mu\gamma)$ in the nondegenerate case for three different choices of SUSY parameters. The parameters (y_1,y_2,y_3,θ) are randomly generated within the designated range.

shown in Fig. 6, $\mathcal{B}(\mu \to e\gamma)$ is larger for larger y_1 and $\mathcal{B}(\tau \to \mu\gamma)$ mainly depends on y_2.

In Fig. 7, we present a scatter plot of $\mathcal{B}(\mu \to e\gamma)$ and $\mathcal{B}(\tau \to \mu\gamma)$ for different choices of SUSY parameters:

(i) $A_0 = -2$, $M_0 = 2$ TeV, and $\tan\beta = 30$;
(ii) $A_0 = 0$, $M_0 = 6$ TeV, and $\tan\beta = 30$;
(iii) $A_0 = 0$, $M_0 = 6$ TeV, and $\tan\beta = 50$;

with $M_{1/2} = 1.5$ TeV and $\mu > 0$, where the parameters in the neutrino Yukawa matrix are randomly varied as indicated. These choices satisfy the experimental constraints and give $m_h \simeq 126$ GeV. The choice (i) is the same as the plot in Fig. 5. For the choice (ii), A_0 is set to zero, and thus the large value of $M_0 = 6$ TeV is required to reproduce the observed Higgs boson mass. Accordingly, both $\mathcal{B}(\mu \to e\gamma)$ and $\mathcal{B}(\tau \to \mu\gamma)$ are suppressed because of larger slepton masses. For the choice (iii), the large $\tan\beta$ increases $\mathcal{B}(\mu \to e\gamma)$ and $\mathcal{B}(\tau \to \mu\gamma)$, and the latter can be as large as 5×10^{-10} within $y_2, y_3 < 2.0$. We note that $y_2, y_3 \simeq 2.0$ gives the value of the heaviest right-handed neutrino mass close to the GUT scale. In all these cases, $\mathcal{B}(\mu \to e\gamma)$ can be larger than 5×10^{-14} if y_1 is close to 0.1.

V. SUMMARY AND CONCLUSION

We have studied the lepton flavor violation in the supersymmetric seesaw model of type I with the ansatz from the minimal supergravity. We have evaluated the latest constraints on the SUSY parameters, taking into account recent experimental improvements for the Higgs boson mass and direct searches of the SUSY particles at the LHC, the rare decay of $B_s \to \mu^+\mu^-$ in the dedicated B experiments, the neutrino mixing angle of θ_{13} in the neutrino experiments, and the charged lepton-flavor-violating decay in the MEG experiment. The Higgs boson mass strongly constrains the SUSY parameters, and we have shown that the allowed region of the universal scalar mass M_0 and gaugino mass $M_{1/2}$ depends on the universal trilinear coupling A_0 as shown in Figs. 1 and 2. We have also found that the constraints from the B physics are important, because $\mathcal{B}(\bar{B} \to X_s\gamma)$ gives the strong constraint in a certain parameter region.

Using the obtained allowed region of the SUSY parameters, we have investigated the effect of the parameters in the neutrino Yukawa matrix Y_N and Majorana mass matrix M_N on the LFV decays $\tau \to \mu\gamma$ and $\mu \to e\gamma$. In this study, we considered the degenerate and nondegenerate cases for Y_N and M_N. In the degenerate case, M_N is assumed to be proportional to the unit matrix. We have found that $\mathcal{B}(\tau \to \mu\gamma)$ is less than 2×10^{-12} for $O_N = \mathbf{1}$ with the present bound of $\mathcal{B}(\mu \to e\gamma)$ and the current experimental value of $\sin^2\theta_{13}$. However, $\mathcal{B}(\tau \to \mu\gamma)$ can be larger than 10^{-9} when the CP-violating parameters in O_N are taken into account together with the CP-violating phases in U_ν. In the nondegenerate case, we assume that Y_N has a mixing only between the second and third generations. In this case, $\mathcal{B}(\mu \to e\gamma)$ and $\mathcal{B}(\tau \to \mu\gamma)$ depend on the different parameters in Y_N. We have found that $\mathcal{B}(\tau \to \mu\gamma)$ can be larger than 10^{-9} for $A_0 = -2$. For a smaller value of $|A_0|$, the branching ratio is smaller because of the required large masses of sleptons.

The future experiment at SuperKEKB/Belle II is able to search for $\tau \to \mu\gamma$ down to $\mathcal{B}(\tau \to \mu\gamma) \sim 10^{-9}$ [31]. In our analysis, $\mathcal{B}(\tau \to \mu\gamma) > 10^{-9}$ can be obtained for both degenerate and nondegenerate cases. For the search for muon LFV processes, several new and upgraded experiments are now under construction. The MEG II experiment [32] can reach a sensitivity down to $\mathcal{B}(\mu \to e\gamma) \simeq 5 \times 10^{-14}$. The phase II COMET experiment [58] and the Mu2e experiment [59] can reach to $\mathcal{B}(\mu^- N \to e^- N) \sim 10^{-17}$–$10^{-18}$, which corresponds to $\mathcal{B}(\mu \to e\gamma) \sim 10^{-14} - 10^{-15}$ in the SUSY seesaw model where the photon dipole operator gives dominant contributions. Thus, the future experiments for the μ-e conversion search will be also useful to investigate the SUSY seesaw model.

In conclusion, the SUSY seesaw model in the context of the minimal supergravity is a viable new physics candidate that is consistent with the observed Higgs boson mass and other new physics searches. The exploration of LFV processes at the intensity frontier may provide us with the signal of the SUSY seesaw model in conjunction with the new physics search at the energy frontier.

ACKNOWLEDGMENTS

We are grateful to Werner Porod for a helpful comment on the renormalization group running in the public code of SPheno. This work is supported in part by JSPS KAKENHI, Grants No. 20244037 and No. 22244031 for Y. O., No. 23104011 and No. 24340046 for T. S., No. 25400257 for M. T., and by IBS-R018-D1 for R. W.

[1] B. T. Cleveland, T. Daily, R. Davis, Jr., J. R. Distel, K. Lande, C. K. Lee, P. S. Wildenhain, and J. Ullman, Astrophys. J. **496**, 505 (1998); Y. Fukuda *et al.* (Kamiokande Collaboration), Phys. Rev. Lett. **77**, 1683 (1996); J. N. Abdurashitov *et al.* (SAGE Collaboration), J. Exp. Theor. Phys. **95**, 181 (2002); T. Kirsten *et al.* (GALLEX Collaboration and GNO Collaboration), Nucl. Phys. B, Proc. Suppl. **118**, 33 (2003); C. Cattadori, N. Ferrari, and L. Pandola, Nucl. Phys. B, Proc. Suppl. **143**, 3 (2005).

[2] P. Minkowski, Phys. Lett. **67B**, 421 (1977); M. Gell-Mann, P. Ramond, and R. Slansky, *Proceedings of the Supergravity Stony Brook Workshop, New York, 1979*, edited by P. Van Nieuwenhuizen and D. Freedman (North-Holland, Amsterdam, 1979); T. Yanagida, *Proceedings of the Workshop on Unified Theories and Baryon Number in the Universe, Tsukuba, Japan, 1979*, edited by A. Sawada and A. Sugamoto (KEK Report No. 79-18, 1979); R. N. Mohapatra and G. Senjanovic, Phys. Rev. Lett. **44**, 912 (1980).

[3] F. Borzumati and A. Masiero, Phys. Rev. Lett. **57**, 961 (1986).

[4] G. Aad *et al.* (ATLAS Collaboration), Phys. Lett. B **716**, 1 (2012).

[5] S. Chatrchyan *et al.* (CMS Collaboration), Phys. Lett. B **716**, 30 (2012).

[6] G. Aad *et al.* (ATLAS Collaboration), Phys. Rev. D **90**, 052004 (2014).

[7] S. Chatrchyan *et al.* (CMS Collaboration), Report No. CMS-PAS-HIG-14-009.

[8] G. Aad *et al.* (ATLAS Collaboration), J. High Energy Phys. 10 (2013) 130; 01 (2014) 109(E); Report No. ATLAS-CONF-2013-047; Report No. ATLAS-CONF-2013-061; Report No. ATLAS-CONF-2013-062.

[9] S. Chatrchyan *et al.* (CMS Collaboration), Report No. CMS-SUS-12-024; Report No. CMS-SUS-12-028; Report No. CMS-SUS-13-004; Report No. CMS-SUS-13-007; Report No. CMS-SUS-13-008; Report No. CMS-SUS-13-013.

[10] Y. Amhis *et al.* (HFAG Collaboration), arXiv:1207.1158, and online update at http://www.slac.stanford.edu/xorg/hfag/.

[11] R. Aaij *et al.* (LHCb Collaboration), Phys. Rev. Lett. **110**, 021801 (2013).

[12] V. Khachatryan *et al.* (CMS and LHCb collaborations), arXiv:1411.4413.

[13] R. Aaij *et al.* (LHCb Collaboration), Phys. Rev. Lett. **111**, 101805 (2013).

[14] S. Chatrchyan *et al.* (CMS Collaboration), Phys. Rev. Lett. **111**, 101804 (2013).

[15] B. Pontecorvo, Sov. Phys. JETP **6**, 429 (1957); **7**, 172 (1958); **26**, 984 (1968); Z. Maki, M. Nakagawa, and S. Sakata, Prog. Theor. Phys. **28**, 870 (1962).

[16] K. Olive *et al.* (Particle Data Group), Chin. Phys. C **38**, 090001 (2014).

[17] K. Abe *et al.* (T2K Collaboration), Phys. Rev. Lett. **107**, 041801 (2011); Phys. Rev. D **88**, 032002 (2013).

[18] P. Adamson *et al.* (MINOS Collaboration), Phys. Rev. Lett. **107**, 181802 (2011).

[19] Y. Abe *et al.* (Double Chooz Collaboration), Phys. Rev. Lett. **108**, 131801 (2012); Phys. Rev. D **86**, 052008 (2012).

[20] F. P. An *et al.* (Daya Bay Collaboration), Phys. Rev. Lett. **108**, 171803 (2012); Chin. Phys. C **37**, 011001 (2013).

[21] J. K. Ahn *et al.* (RENO Collaboration), Phys. Rev. Lett. **108**, 191802 (2012).

[22] J. Adam *et al.* (MEG Collaboration), Phys. Rev. Lett. **110**, 201801 (2013).

[23] B. Aubert *et al.* (*BABAR* Collaboration), Phys. Rev. Lett. **104**, 021802 (2010).

[24] K. Hayasaka *et al.* (Belle Collaboration), Phys. Lett. B **666**, 16 (2008).

[25] T. Goto, Y. Okada, T. Shindou, and M. Tanaka, Phys. Rev. D **77**, 095010 (2008).

[26] S. T. Petcov and T. Shindou, Phys. Rev. D **74**, 073006 (2006).

[27] F. Deppisch, H. Pas, A. Redelbach, and R. Ruckl, Phys. Rev. D **73**, 033004 (2006); S. T. Petcov, W. Rodejohann, T. Shindou, and Y. Takanishi, Nucl. Phys. **B739**, 208 (2006); S. Antusch, E. Arganda, M. J. Herrero, and A. M. Teixeira, J. High Energy Phys. 11 (2006) 090; E. Arganda, M. J. Herrero, and J. Portoles, J. High Energy Phys. 06 (2008) 079; M. Hirsch, J. W. F. Valle, W. Porod, J. C. Romao, and A. Villanova del Moral, Phys. Rev. D **78**, 013006 (2008); M. J. Herrero, J. Portoles, and A. M. Rodriguez-Sanchez, Phys. Rev. D **80**, 015023 (2009); A. Abada, A. J. R. Figueiredo, J. C. Romao, and A. M. Teixeira, J. High Energy Phys. 10 (2010) 104.

[28] M. Hirsch, F. R. Joaquim, and A. Vicente, J. High Energy Phys. 11 (2012) 105; T. Moroi, M. Nagai, and T. T. Yanagida, Phys. Lett. B **728**, 342 (2014); J. H. Park, Phys. Rev. D **89**, 095005 (2014).

[29] A. J. R. Figueiredo and A. M. Teixeira, J. High Energy Phys. 01 (2014) 015.

[30] L. Calibbi, D. Chowdhury, A. Masiero, K. M. Patel, and S. K. Vempati, J. High Energy Phys. 11 (2012) 040.

[31] T. Aushev *et al.*, arXiv:1002.5012.

[32] A. M. Baldini *et al.* (MEG Collaboration), arXiv:1301.7225.

[33] P. Z. Skands *et al.*, J. High Energy Phys. 07 (2004) 036; B. C. Allanach *et al.*, Comput. Phys. Commun. **180**, 8 (2009); G. Brooijmans *et al.*, arXiv:1203.1488; F. Mahmoudi *et al.*, Comput. Phys. Commun. **183**, 285 (2012).

[34] N. Cabibbo, Phys. Rev. Lett. **10**, 531 (1963); M. Kobayashi and T. Maskawa, Prog. Theor. Phys. **49**, 652 (1973).

[35] J. A. Casas and A. Ibarra, Nucl. Phys. **B618**, 171 (2001).

[36] W. Porod, Comput. Phys. Commun. **153**, 275 (2003); W. Porod and F. Staub, Comput. Phys. Commun. **183**, 2458 (2012).

[37] J. R. Ellis, S. Ferrara, and D. V. Nanopoulos, Phys. Lett. **114B**, 231 (1982); M. Pospelov and A. Ritz, Ann. Phys. (Amsterdam) **318**, 119 (2005).

[38] S. Antusch, J. Kersten, M. Lindner, M. Ratz, and M. A. Schmidt, J. High Energy Phys. 03 (2005) 024.

[39] J. Ellis, A. Hektor, M. Kadastik, K. Kannike, and M. Raidal, Phys. Lett. B **631**, 32 (2005).

[40] A. Bartl, W. Majerotto, W. Porod, and D. Wyler, Phys. Rev. D **68**, 053005 (2003).

[41] J. Hisano, T. Moroi, K. Tobe, and M. Yamaguchi, Phys. Rev. D **53**, 2442 (1996).

[42] A. J. Buras, P. H. Chankowski, J. Rosiek, and L. Slawianowska, Nucl. Phys. **B659**, 3 (2003).

[43] E. Lunghi and J. Matias, J. High Energy Phys. 04 (2007) 058.

[44] Y. Okada, M. Yamaguchi, and T. Yanagida, Prog. Theor. Phys. **85**, 1 (1991); H. E. Haber and R. Hempfling, Phys. Rev. Lett. **66**, 1815 (1991); J. R. Ellis, G. Ridolfi, and F. Zwirner, Phys. Lett. B **257**, 83 (1991).

[45] A. Dedes, G. Degrassi, and P. Slavich, Nucl. Phys. **B672**, 144 (2003).
[46] P. Adamson *et al.* (MINOS Collaboration), Phys. Rev. Lett. **110**, 171801 (2013).
[47] K. Abe *et al.* (T2K Collaboration), Phys. Rev. Lett. **112**, 061802 (2014).
[48] J. P. Lees *et al.* (*BABAR* Collaboration), Phys. Rev. D **86**, 112008 (2012).
[49] M. Misiak, *et al.*, Phys. Rev. Lett. **98**, 022002 (2007); T. Becher and M. Neubert, Phys. Rev. Lett. **98**, 022003 (2007).
[50] F. Jegerlehner and A. Nyffeler, Phys. Rep. **477**, 1 (2009); M. Davier, A. Hoecker, B. Malaescu, and Z. Zhang, Eur. Phys. J. C **71**, 1515 (2011); K. Hagiwara, R. Liao, A. D. Martin, D. Nomura, and T. Teubner, J. Phys. G **38**, 085003 (2011).
[51] G. Bennett *et al.* (Muon G-2 Collaboration), Phys. Rev. D **73**, 072003 (2006).
[52] M. Endo, K. Hamaguchi, S. Iwamoto, and N. Yokozaki, Phys. Rev. D **84**, 075017 (2011); **85**, 095012 (2012).
[53] R. Kitano, M. Koike, and Y. Okada, Phys. Rev. D **66**, 096002 (2002); **76**, 059902 (2007); R. Kitano, M. Koike, S. Komine, and Y. Okada, Phys. Lett. B **575**, 300 (2003); V. Cirigliano, R. Kitano, Y. Okada, and P. Tuzon, Phys. Rev. D **80**, 013002 (2009).
[54] C. Dohmen *et al.* (SINDRUM II Collaboration), Phys. Lett. B **317**, 631 (1993); W. Honecker *et al.* (SINDRUM II Collaboration), Phys. Rev. Lett. **76**, 200 (1996); W. H. Bertl *et al.* (SINDRUM II Collaboration), Eur. Phys. J. C **47**, 337 (2006).
[55] S. Chatrchyan *et al.* (CMS Collaboration), Report No. CMS-PAS-HIG-14-005.
[56] E. Arganda, A. M. Curiel, M. J. Herrero, and D. Temes, Phys. Rev. D **71**, 035011 (2005).
[57] A. Himmel *et al.* (Super Kamiokande Collaboration), AIP Conf. Proc. **1604**, 345 (2014).
[58] Y. G. Cui *et al.* (COMET Collaboration), Report No. KEK-2009-10.
[59] R. J. Abrams *et al.* (Mu2e Collaboration), arXiv:1211.7019.